ISSN (Print) 1226-1750
ISSN (Online) 2233-6656
Journal of Magnetics 24(3), 485-490 (2019) https://doi.org/10.4283/JMAG.2019.24.3.485

Improving the Magnetic Properties of FeSiB Soft Magnetic Composites by Adding Untreated or Phosphated Fe Powders

D. N. Chen, L. Huang, H. Y. Yu*, X. C. Zhong, and Z. W. Liu

School of Materials Science and Engineering, South China University of Technology, Guangzhou 510640, China

(Received 20 January 2019, Received in final form 29 June 2019, Accepted 2 July 2019)

Soft magnetic composites (SMC) based on FeSiB amorphous alloys have been widely used in various electric devices. However, the amorphous powders are difficult to press, and the prepared cores exhibit low mechanical strength with high porosity. In this work, untreated and phosphated Fe powders with mean particle size of 70 μm were added into FeSiB powders with mean size of less than 25 μm to improve the performance of the SMC. The FeSiB/Fe SMCs are fabricated by cold pressing. The results show that the amplitude permeability of FeSiB/Fe SMCs increases with the increase of Fe content. However, the addition of untreated Fe powder leads to increased magnetic loss. On the contrary, the addition of phosphated iron powder can not only enhance the amplitude permeability but also effectively reduce the core loss. Hence, the addition of phosphated iron powder provides a good way to modify the soft magnetic properties of FeSiB/Fe SMC for AC application.

Keywords : FeSiB soft magnetic composite, Fe powder, phosphorization, amplitude permeability, magnetic loss

1. Introduction

Iron based amorphous powder cores with excellent soft magnetic properties, including high permeability, high electrical resistivity, low coercivity, and stress insensitivity, are widely used for various electrical and electronic devices with small size, light weight and high frequency stability [1-3]. Recently, much effort has been devoted to studying the processing and magnetic properties of various kinds of Fe-Si-M powder cores [4] such as FeSiB, FeSiNbBCu [5-7], FeSiCr [8, 9] and FeSiAl [10]. Compared to FeSiNbBCu and FeSiAl powder cores, FeSiB amorphous cores have simpler composition, better DC magnetic properties, and higher saturation magnetization, thus attracting much attention from both academic and industry.

The preparation of FeSiB soft magnetic composites (SMC) involves passive treatment [11], organic coating [12, 13], mold forming [14] and annealing treatment [15, 16], etc. The initial FeSiB amorphous powders are too brittle to compact into complex shape. The binder like silicone is important for the core forming and for the formation of an organic layer on the metallic powders. Generally, a high silicone content can effectively increase the resistivity of FeSiB amorphous powder, but it also decreases the saturation magnetization and the mechanical strength. In addition, the curing temperature must be lower than the decomposition temperature of organic binder. The lack of high temperature annealing during preparation may be one of the reasons for the low mechanical strength of FeSiB SMCs. On the other hand, FeSiB SMCs have high porosity due to the huge difference in thermal expansion coefficient between the organic binder and the metallic powder. Hence, in the recent years, much attention has been focused on increasing the density by improving the compact technology and decreasing the eddy current loss under high frequency for FeSiB soft magnetic composite.

It was demonstrated that the properties of FeSiB SMCs can be effectively enhanced by mixing FeSiB amorphous powder with permalloy powder [17], soft ferrite [18], and iron powder [19]. It was reported that addition of permalloy powder [17] is helpful for compaction of the FeSiB SMCs. The magnetic permeability of FeSiB SMCs can be enhanced by adding permalloy powder, but the eddy current loss increases with the increasing content of permalloy powder. The high cost of permalloy powder also increases the production cost of SMCs. Li *et al.* [18] found that the addition of ferrite is beneficial for both magnetic permeability and magnetic loss. Compared with

*Corresponding author: Tel: +86-20-22236906
Fax: +86-20-22236906, e-mail: yuhongya@scut.edu.cn

FeSiB CMC, FeSiB SMC added with 2 wt.% (NiZn)Fe_2O_4 nanoparticles exhibited 44 % higher permeability and maintained a relatively low eddy current loss under high frequency. Kim *et al.* [19] reported that the SMC made from the mixture of FeSiB amorphous powder and pure iron powder exhibit high density and excellent magnetic properties. However, adding pure iron powder was found to results in an increase of magnetic core loss.

Considering the low cost and excellent engineering properties such as low hardness, good compactability, and superior magnetic properties, iron powder is indeed a good addition for improving the combination of magnetic properties of FeSiB SMC. Its magnetic loss, in particular the eddy current loss, may be reduced by improving the insulation of the powder. Hence, in this work, aiming to improve both amplitude permeability and magnetic loss, the effects of untreated and phosphated iron powders additions on the soft magnetic properties of Fe/FeSiB magnetic composites have been investigated.

2. Experimental

The gas-atomized FeSiB amorphous powders and the pure reduced iron powders were used in this study. The amorphous powder consists of 2.8 wt.% B, 5.5 wt.% Si, and balanced Fe. The average size of the amorphous powder is less than 25 μm. The purity of the Fe is over 99 wt.% with 0.008 wt.% C and 0.005 wt.% S. The average size of the pure iron powder is less than 75 μm. The silicone resin is used as binder agent. To prepare the SMC cores, 3 wt.% silicon resin was firstly dissolved into 20 ml acetone solution. Both untreated iron powders and phosphate iron powders were used for fabricating SMCs. For phosphorization, 20 g iron powders were added to 3.0 wt.% phosphatic acid acetone solution (20 ml) and stirred at room temperature for 30 minutes. The wet phosphatized iron powders were washed repeatedly by deionized water for two times and cleaned by alcohol. After that, the cleaned phosphatized iron powders were dried at 120 °C for 2 hours. For preparing SMCs, FeSiB amorphous powders and untreated Fe powders or phosphated Fe powders with various weight ratios were mixed in a ball miller with a rotation speed of 120 r/min. The powder mixture was stirred in the solution until the solution completely evaporated. The powder mixture was put into a vacuum oven and dried at 80 °C for two hours. Toroid-shaped FeSiB composite powder cores with outer diameter of 20 mm, inner diameter of 12 mm and height of 4 mm were prepared by cold pressing under a pressure of 1200 MPa. Finally, all composite cores were annealed under argon atmosphere for an hour to release the internal stress caused by pressing. Two distinction groups were studied based on untreated iron powder and phosphated iron powder.

The structure of the powder was analyzed by X-ray diffraction (XRD) using Cu Kα-radiation. The morphology and magnetic properties for the samples were analyzed by the scanning electron probe microscopy (SEM) and physical property measurement system (PPMS). The thermal behavior was determined using differential scanning calorimeter (DSC).

The amplitude permeability and the core loss of composite powder cores were measured by a soft magnetic alternating current test device (MATS-2010SA).

3. Results and Discussion

The XRD patterns for amorphous FeSiB powder and reduced Fe powder are shown in Fig. 1(a). The FeSiB pattern shows a diffuse peak confirming the amorphous structure. The inset patterns for Fe powder has three sharp and intense peaks at about 44.7º, 65.0º, and 82.4º, corre-

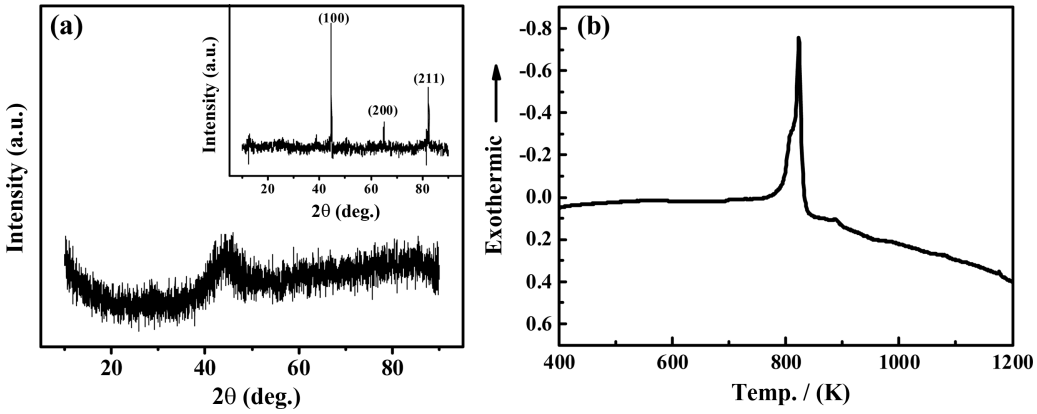

Fig. 1. XRD patterns of FeSiB amorphous powder and reduced iron powder (inset) (a), and DSC curve of FeSiB amorphous powder (b).

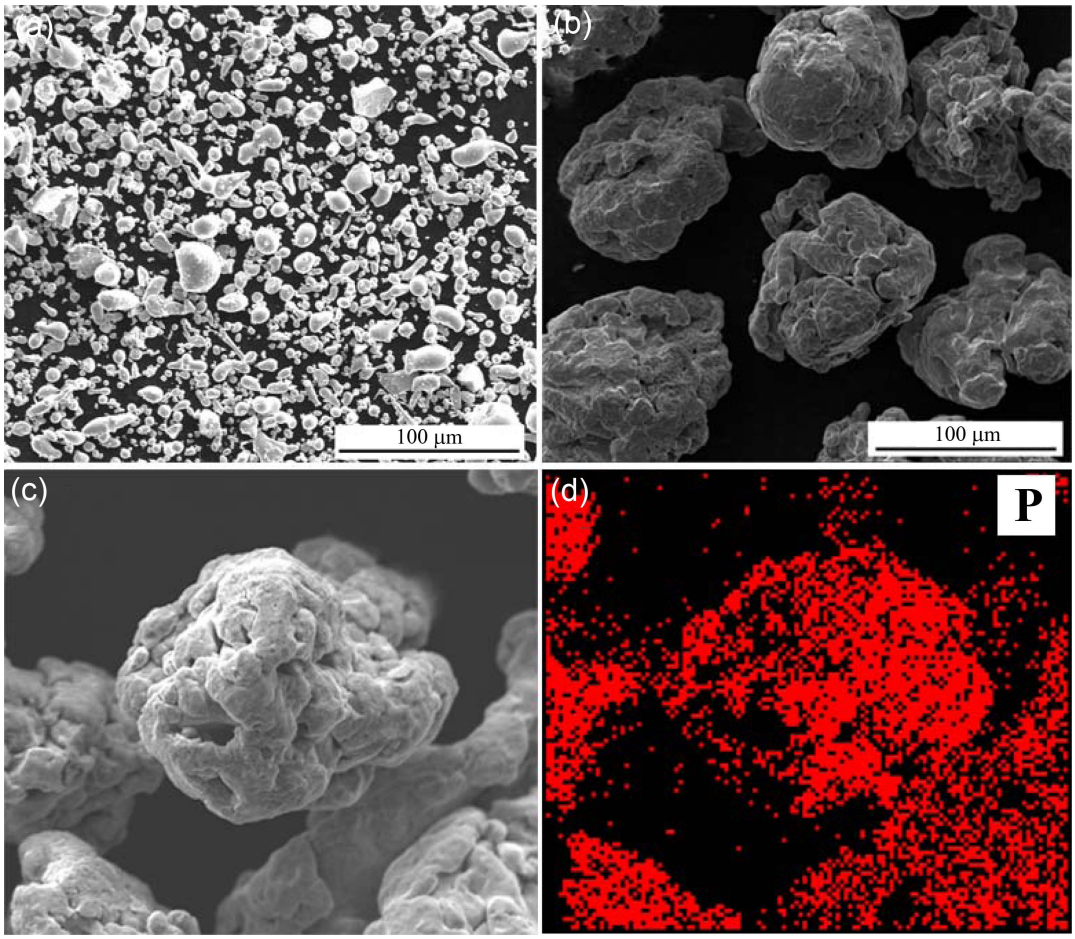

Fig. 2. (Color online) SEM images of FeSiB amorphous powder (a) and Fe powder (b). The microstructure (c) and P element EDS mapping of the Fe powders after phosphating (d).

sponding to (100), (200), and (211) of α-Fe, respectively. Fig. 1(b) shows the DSC curve of FeSiB powder. The onset temperature of primary crystallization and final crystallization temperature are about 773 K and 847 K, respectively. Based on DSC result, the annealing of FeSiB amorphous powder will be carried out at 723 K to avoid crystallization.

The SEM images for FeSiB amorphous powders and iron powders are shown in Fig. 2(a) and (b), respectively. The iron powders exhibit a rough and irregular surface, while the shape of most gas-atomized FeSiB amorphous powders are spherical except some large particles, which is suitable for core formation and protecting insulating coating from breaking. As we know, the value of eddy current loss is inverse proportional to the electrical resistivity and proportional to the density of the materials [20, 21]. To increase the electric resistance and reduce the eddy current loss, chemistry treatment with phosphoric acid was employed to modify the surface of the iron powder. EDS image in Fig. 2(c) and (d) shows the distribution of P element on the Fe powders after phosphating. P is uniformly coated on the surface, indicating that phosphating layer has been formed. It was reported by Hsiang *et al.* [22] that when the concentration of the phosphoric acid changed from 1 wt.% to 2 wt.%, the thickness of inorganic insulation on carbonyl iron core increased from 30 to 60 nm. The phosphorization can not only increase the resistivity but also improve the interaction with silicon resin and iron powder.

The hysteresis loops for FeSiB amorphous powder and Fe powder are shown in Fig. 3. Both powders exhibit very good soft magnetic properties with very low coercivity. The saturation magnetization of FeSiB and Fe powder are 158.6 emu/g and 187.5 emu/g, respectively. The initial permeability of Fe powder is higher than that of FeSiB powder.

Fig. 4(a) shows the frequency dependence of the amplitude permeability μ_a of the FeSiB/Fe SMCs with various additions of untreated iron powder. The μ_a, measured at a periodic alternating magnetic field, can be

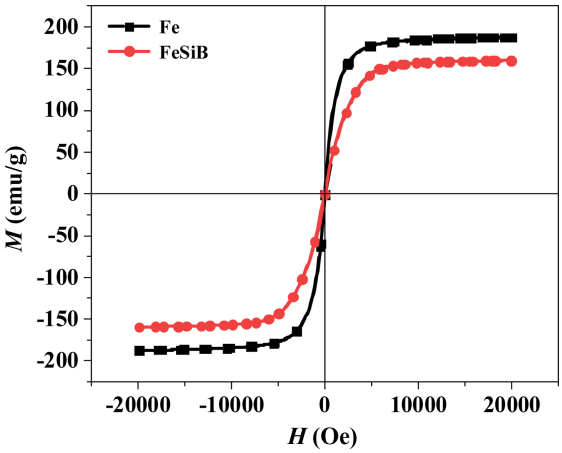

Fig. 3. (Color online) SEM images of FeSiB amorphous powder (a) and Fe powder (b). The microstructure (c) and P element EDS mapping of the Fe poThe hysteresis loops for FeSiB amorphous powder and Fe powder.

expressed by

$$\mu_a = \frac{B_m}{\mu_0 H_m}$$

where μ_0 refers to vacuum permeability, H_m and B_m corresponds to the peak value of magnetic field strength and magnetic flux density, respectively, at any point on the dynamic magnetization curve. All samples have stable amplitude permeability in the frequency range between 10 and 100 kHz. The FeSiB amorphous powder core without iron powder addition exhibits the amplitude permeability around 27.9 under 100 kHz for 50 mT. The amplitude permeability of the SMC increases from 36.3 to 46.7 with increasing iron powder content from 10 wt.% to 30 wt.%. The increased μ_a should be attributed to the higher amplitude permeability of Fe powders than FeSiB powders. However, Fig. 4(b) shows that the core loss also increases with the iron powder content due to the relatively low resistivity of Fe powders, which leads to high eddy current loss.

The frequency dependences of the amplitude permeability for various FeSiB/Fe SMCs are presented in Fig. 4(c). No significant decrease is observed in amplitude permeability for the samples with and without phosphatizing, which demonstrates that the addition of phosphated iron powder has no significant negative effect on the amplitude permeability. The main reasons for the slight

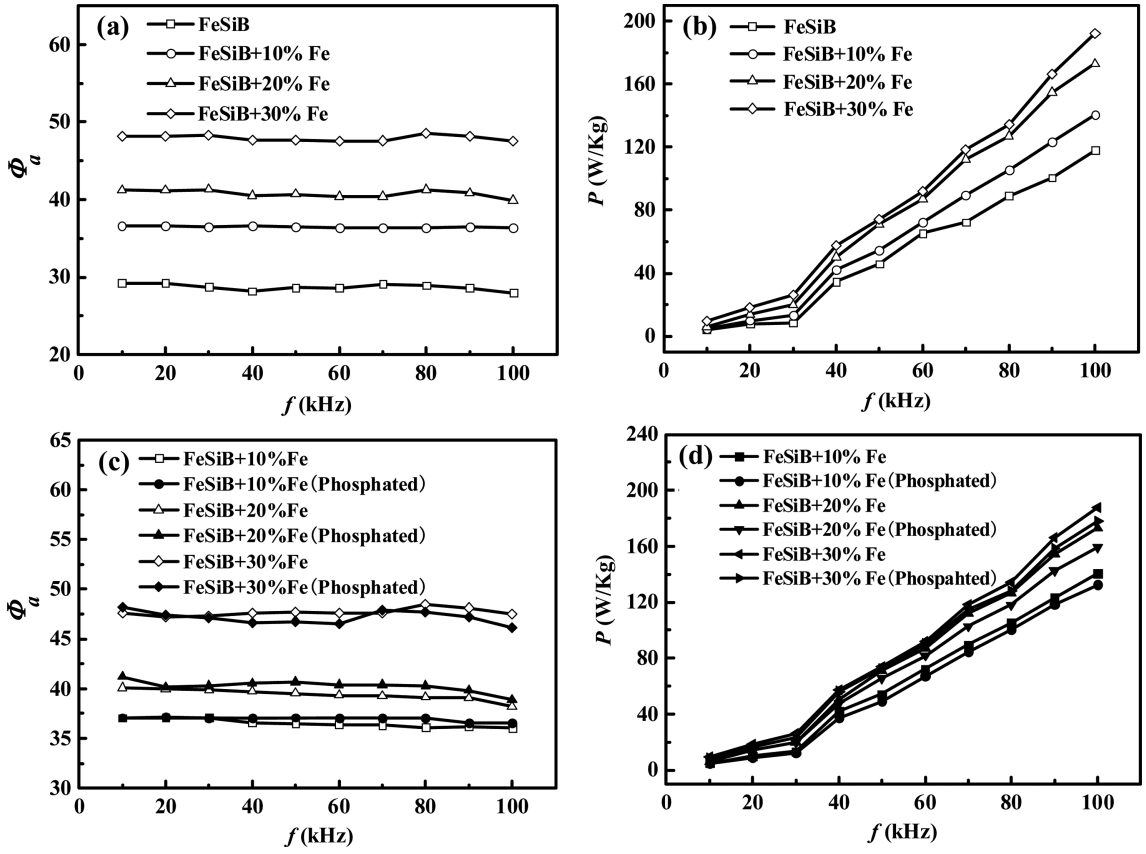

Fig. 4. Frequency dependence of the amplitude permeability, and core loss for FeSiB amorphous powder cores with addition of untreated iron powder ((a) and (c)) and phosphated iron powders ((b) and (d)).

decrease of μ_a can be explained based on non-magnetic particle boundary model, which can be expressed by the equation [23, 24],

$$\mu_{eff} = \frac{D\mu_i}{D + \delta\mu_i}$$

where D denotes diameter of particle, δ is the distance between adjacent magnetic particles, and μ_i represents the initial permeability of magnetic material. After phosphatizing treatment, a relatively uniform, dense and thin surface [25] can be formed on the iron powder. The phosphating surface is considered as the insulating layer, which can separate the magnetic particles from each other to avoid agglomeration. The separation of magnetic particles result in a decrease of induced current, which reduces the eddy current loss under high frequency. In addition, the insulating layer, regarded as a nonmagnetic film with certain thickness of film, results in the increases distance δ of adjacent magnetic particle, which reduces the amplitude permeability. In addition, two effects include loosening effect and wall effect [26-28] are generally used to calculate the packing density of powder in order to choose the suitable ratio of coarse and fine powder ratio. In this work, the particle size ratio of iron powder and FeSiB amorphous powder is about 3.5. The fine FeSiB amorphous powder can enter into porosities between coarse iron powders under the pressure of 1200 MPa. Compared with uncoated iron powder, the FeSiB/Fe SMC with phosphating treatment has higher density, demonstrating the reduced defects. This is also the reason why the amplitude permeability only varied slightly after phosphating.

Fig. 4(d) shows the frequency dependences of the core loss of the SMCs with various additions of phosphated iron powder. The FeSiB amorphous powder cores with 20 wt.% addition of untreated and phosphatized iron powders show a core loss of about 178 W/kg and 159.1 W/kg at 100 kHz for 50 mT, respectively. As we know, theoretically, the eddy current loss, which is dominant under high frequency, can be effectively reduced by insulating treatment. The eddy current loss can be divided into interparticle eddy current loss and intraparticle eddy current loss. Compared with the mixture of uncoated iron powder and FeSiB amorphous powder, the decrease of core loss with phosphated iron powder addition can be explained by the reduced contact of magnetic particle.

Table 1 shows the density and resistivity of the FeSiB/Fe SMC with prepared with untreated and phosphate Fe powders. Compared with FeSiB amorphous powder core with untreated iron powder, FeSiB/Fe SMC with phosphated iron powder has higher density. As we know, the fluidity of powder can be enhanced by the formation of a continuous and smooth insulating layer. During the process of cold pressing, the coarse particle and fine particle with good fluidity are pressed tightly, which leads to an increase in phosphatized Fe/FeSiB SMC. For the samples with untreated Fe powder, the electrical resistivity decreases with the increasing pure iron powder weight, due to the lower resistivity of Fe than Fe-Si-B. Similar variation is also observed for the samples added with phosphated Fe powder. Compared to the samples without phosphorization, the samples added with phosphate Fe powders show higher resistivity due to the integrated inorganic insulation formed on the iron powders.

Table 1. The density and electric resistivity of FeSiB/Fe SMC with prepared with untreated and phosphated Fe powders.

Samples	Density (g/cm^3)	Resistivty (Ω/mm)
0.7FeSiB/0.3Fe	5.83	0.0347
0.8FeSiB/0.2Fe	5.86	0.0451
0.9FeSiB/0.1Fe	5.92	0.0561
0.7FeSiB/0.3Fe (after phosphating)	5.85	0.0632
0.8FeSiB/0.2Fe (after phosphating)	5.96	0.0545
0.9FeSiB/0.1Fe (after phosphating)	5.97	0.0403

4. Conclusion

The amplitude permeability of FeSiB SMC can be effectively enhanced by adding untreated iron powder. Both amplitude permeability and magnetic magnetization of FeSiB/Fe SMC increased with the increase of iron powder content. 30 wt.% Fe powder addition led to 62.3 % increase in the amplitude permeability but also an increase in the core loss. The addition of phosphated iron powder is benefit for decreasing the core loss of Fe/FeSiB amorphous powder and maintaining high amplitude permeability. Compared with the SMC added with untreated Fe powder, the FeSiB SMC with 20 wt.% phosphate Fe powder exhibits 22.5 % decrease in the magnetic core loss at 100 kHz for 50 mT. The present results indicate that adding phosphated Fe powder is a good approach to improve the performance of FeSiB SMC.

Acknowledgement

This work was partly supported by the Mentech Optical and Magnetic Co. Ltd.

References

[1] F. Alves, R. Lebourgeois, and T. Waeckerlé, Int. Trans.

Electr. Energy Syst. **15**, 467 (2010).
[2] Y. G. Guo, J. G. Zhu, P. A. Watterson, and W. Wu, IEEE Trans. Energy Conver. **21**, 426 (2006).
[3] A. M. Leary, P. R. Ohodnicki, and M. E. Mchenry, JOM **64**, 772 (2012).
[4] Y. Cui, J. Zhou, and Y. Xiao, Mater. Rev. **24**, 27 (2010).
[5] M. Müller, A. Novy, M. Brunner, and R. Hilzinger, J. Magn. Magn. Mater. **196**, 357 (1999).
[6] F. Alves, C. Ramiarinjaona, S. Berenguer, R. Lebourgeois, and T. Waeckerle, IEEE Trans. Magn. **38**, 3135 (2002).
[7] S. Yue, H. Zhang, R. Cheng, A. Wang, Y. Dong, A. He, H. G. Ni, and C. T. Liu, J. Alloys Compd. **776**, 833 (2019).
[8] P. Jang and G. Choi, IEEE Trans. Magn. **53**, 1 (2017).
[9] X. L. Zhou, D. F. Liang, and X. Wang, IEEE Trans. Magn. **51**, 1 (2015).
[10] T. D. Zhou, L. J. Deng, and D. F. Liang, Acta Metall. Sin. **21**, 191 (2008).
[11] M. Kabátová, E. Dudrová, and H. Bruncková, Surf. Interface Anal. **45**, 1166 (2013).
[12] J. Li, J. Yu, W. Li, S. Che, J. Zheng, L. Qiao, and Y. Ying, J. Magn. Magn. Mater. **454**, 103 (2018).
[13] B. Zhou, Y. Dong, L. Liu, L. Chang, F. Q. Bi, and X. M. Wang, J. Magn. Magn. Mater. **474**, 1 (2019).
[14] H. Shokrollahi and K. Janghorban, Mater. Sci. Eng. B-Adv. Funct. Solid-State Mater. **134**, 41 (2006).
[15] Y. Dong, Z. Li, M. Liu, C. Chang, F. Li, and X. M. Wang, Mater. Res. Bull. **96**, 160 (2017).
[16] Z. Li, Y. Dong, S. Pauly, C. Chang, R. Wei, F. Li, and X. M. Wang, J. Alloy Compd. **706**, 1 (2017).
[17] Y. B. Kim and K. Y. Kim, IEEE Trans. Magn. **42**, 2802 (2006).
[18] X. Li, Y. Dong, M. Liu, C. Chang, and X. M. Wang, J. Alloy. Compd. **696**, 1323 (2017).
[19] H. J. Kim, S. K. Nam, K. S. Kim, S. C. Yoon, K. Y. Sohn, M. R. Kim, Y. S. Song, and W. W. Park, Jpn. J. Appl. Phys. **51**, 103001 (2012).
[20] P. Kollár, D. Olekšáková, V. Vojtek, J. Füzer, M. Fáberová, and R. Bureš, J. Magn. Magn. Mater. **424**, 245 (2017).
[21] M. F. D. Campos, T. Yonamine, M. Fukuhara, F. J. G. Landgraf, C. A. Achete, and F. P. Missell, IEEE Trans. Magn. **42**, 2812 (2006).
[22] H. I. Hsiang, L. F. Fan, and J. J. Hung, J. Magn. Magn. Mater. **447**, 1 (2018).
[23] M. T. Johnson and E. G. Visser, IEEE Trans. Magn. **26**, 1987 (1990).
[24] F. Mazaleyrat, V. Leger, R. Lebourgeois, and R. Barrue, IEEE Trans. Magn. **38**, 3132 (2002).
[25] M. Huang, C. Wu, Y. Jiang, and M. Yan, J. Alloy Compd. **644**, 124 (2015).
[26] V. Wong and A. K. H. Kwan, Powder Technol. **268**, 357 (2014).
[27] X. Ye, Y. Li, Y. Ai, and Y. Nie, Adv. Powder Technol. **29**, 2280 (2018).
[28] A. K. H. Kwan, K. W. Chan, and V. Wong, Powder Technol. **237**, 172 (2013).